MODELING AND DESIGN OF A GIFFARD INJECTOR-PUMPED BIPROPELLANT MICROROCKET

Natalya A. Brikner, William G. Gardner, Ivan W. Wang, Jonathan M. Protz*
Mechanical Engineering and Materials Science Department, Duke University, Durham, United States
*Presenting Author: jonathan.protz@duke.edu

Abstract: A design of a bipropellant micro rocket engine is investigated. The proposed engine implements steam-driven injectors in place of turbomachinery for onboard propellant pressurization. The work performed builds on the authors' previous model that showed Giffard injectors to be capable of supplying the high pressures required by microrocket combustion chambers and found the computed performance of the injector-pumped engine comparable to current technologies. Detailed heat transfer analyses predict losses due to friction and boundary layer blockage. In general, the results show that the theory agrees with the experimental results within 15% and the injectors can deliver output pressures up to twice the supplied pressure.

Keywords: rocket, bipropellant, steam injector, heat transfer

NOMENCLATURE

C_D =	restrictor discharge coefficient
C_{drag} =	drag force coefficient
C_f =	friction coefficient
d =	combining cone exit
e =	exit
m =	motive
$\dot{m}$ =	mass flow rate [kg/s]
s =	suction
u =	velocity [m/s]
Δ =	cantilever deflection [mm]
δ =	boundary layer thickness [mm]
δ^* =	boundary layer displacement [mm]
π =	pressure ratio

INTRODUCTION

A successfully designed microrocket could enable active propulsion for micro-spacecraft, offer a complement to or replacement for the main propulsion systems on larger spacecraft, or carry a small payload into orbit. Using injectors for propellant pressurization onboard a microrocket as first introduced by Refs [1, 2] allows the entire engine to be free of moving parts. As part of an ongoing study of the design discussed here, a more complete injector analysis is presented.

Three injectors are implemented in the microrocket design: two that pump the fuel and oxidizer—ethanol and hydrogen peroxide, respectively—and one that pumps water, to be used as the coolant. The small scale of the passages results in significant viscous interactions. These loss mechanisms are modeled using first principles and validated by experiment. The theoretical model developed in this paper will provide a more accurate assessment of the performance of the injector-pumped design.

BACKGROUND

Giffard Injectors

In 1858 Henri Giffard invented the injector as a replacement for the mechanical pumps used to supply the boilers of steam locomotives with feed-water [3]. Supplying a boiler that reaches P_{boiler} during operation with feed-water requires that $P_{feed\text{-}water} \geq P_{boiler}$. Unlike mechanical pumps, the steam injector could pump the feed-water from its tank to the necessary pressures without requiring any moving parts. It afforded designers crude manufacturing tolerances and delivered feed-water without the temperature and pressure fluctuations [4] inherent in the mechanical pumps it replaced, making it the pumping method of choice onboard steam locomotives. A basic schematic of the injector implemented in this design is shown in Fig. 1.

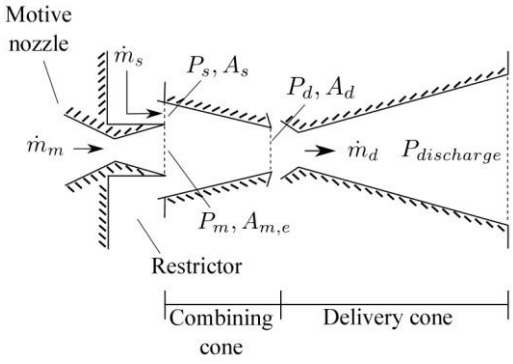

Fig. 1: Schematic of injector as implemented in design.

The injector is supplied with high-pressure motive vapor through a converging-diverging nozzle. At the motive nozzle exit the low-pressure region draws the suction liquid through the restrictor from the tank. The fluids combine and exit the combining cone as a liquid. The mixture is slowed through the delivery cone, recovering dynamic head [3, 5]. A properly designed injector is capable of achieving discharge pressures equal to or greater than the pressure of the supplied motive vapor.

Microrocket Engines

Work on microrockets began in the 1990s at the Massachusetts Institute of Technology [6]. Following

the square-cube law, the thrust-to-weight ratio of a microrocket increases with the inverse of the nozzle throat diameter, implying that rockets at the micro scale can produce T/W ratios up to 100 times that of conventional engines. Components of microrocket engines have been successfully tested, demonstrating the feasibility of chemical rockets on the order of 20 x 5 x 10 mm [7, 8].

Previous Work

The basic injector model used here was first developed by Gardner et al. [9]. The current model has since been adapted for pumping with unlike suction and motive fluids [10]; it now includes the momentum of the suction liquid that was previously assumed to be negligible [10, 11]; and it has been integrated into the microrocket engine in a manner similar to that discussed here and in Ref [10].

The theoretical performance of the proposed injector-pumped microrocket was compared to a similarly designed turbopumped microrocket studied by Protz [7]. Results showed that the performance of the two designs was comparable [10], with computed thrust and specific impulse values from 5-10 N and 250-300 sec, respectively.

ENGINE CYCLE

Several combinations of propellant flow paths, component arrangements, and cooling systems have been considered that (1) provide the motivating vapor to drive the injectors; (2) recover the thermal energy released from decomposition, combustion, and flow through the nozzle; and (3) simplify the propellant injection/ignition in the combustion chamber.

The regenerative cooling decomposition topping cycle shown in Fig. 2 is selected as most suitable, particularly because the cooling relief is provided by a third fluid (water) so that mixing or superheating the fuel and oxidizer prematurely can be avoided. Ethanol and hydrogen peroxide are selected as the fuel and oxidizer, respectively, although other propellant combinations showed satisfactory performance as well [2].

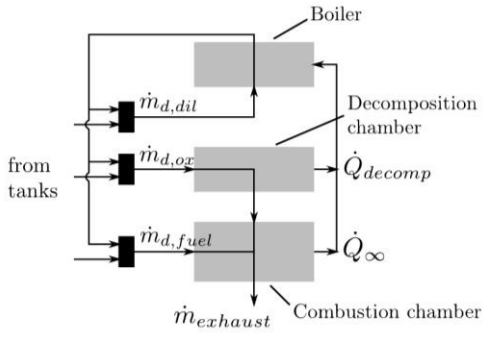

Fig. 2: Schematic of regenerative cooling decomposition topping cycle showing propellant flow paths and main components.

The fuel, oxidizer, and coolant are pumped from their tanks by the vaporized coolant. The oxidizer enters the decomposition chamber where it is introduced to a catalyst that initiates its decomposition. The fuel is injected into the combustion chamber where it joins the gaseous products of H_2O_2 decomposition. The engine cycle is designed such that the heat from decomposition, combustion, and flow through the nozzle will vaporize the coolant in the boiler as shown in Fig. 2, thereby supplying the steam used to motivate the three injectors.

Similar to turbopumped designs, the pressure ratio across the injector is directly related to the chamber pressure of the engine. The injectors are implemented in the design such that

$$P_{chamber} = \pi_{plate} P_{t,discharge} \quad (1)$$

and

$$P_{t,m} = P_{t,discharge} \quad (2)$$

INJECTOR MODEL

Performance and Size

The injectors are designed following the process outlined in Ref [10] for desired performance which allows the injector area ratios to be computed for a specified discharge pressure (neglecting losses). Similarly, for a given injector geometry, the output pressure can be computed.

Losses

In micro-engine channels, widths on the order of micrometers are subject to larger-than-normal viscous forces [13] compared to those acting in macro channels, resulting in increased boundary layer interactions. Two loss mechanisms are studied here: boundary layer blockage and friction. An injector loss model is developed that predicts the injector performance taking into account smaller effective areas and a loss in streamwise momentum.

The boundary layer thickness—given in its general form for flow over a flat plate as

$$\frac{\delta}{x} = C\,Re^{-m} \quad (3)$$

grows proportionally to L^m where m = 0.5 or 0.2 for laminar or turbulent flow, respectively [13]. For high aspect ratio channels the influence of the boundary layer on the inviscid region can no longer be neglected and the actual channel width can be represented in terms of the displacement thickness and effective channel width as in Fig. 3.

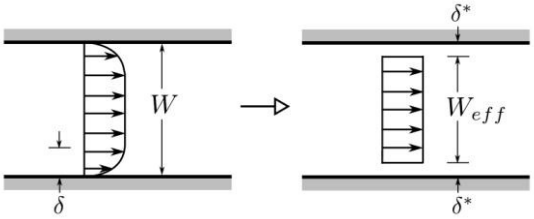

Fig. 3: Representation of actual channel width in terms of effective channel width and boundary layer thickness, adapted from Ref [13].

To compute the displacement due to the boundary layers in the motive nozzle and combining cone, both passages are approximated by parallel flat plates so that the passage width is effectively reduced by $2\delta^*$. Using the appropriate laminar and turbulent correlations for δ^* from Ref [13] the predicted ratios of effective-to-actual area for the motive nozzle and combining cone as functions of chamber pressure are plotted in Fig. 4.

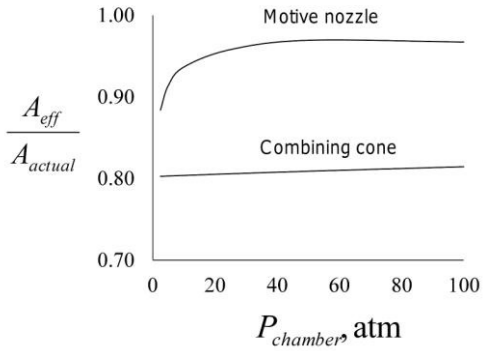

Fig. 4: Reduction in area due to boundary layer displacement as functions of chamber pressure.

At lower chamber pressures, laminar Reynolds numbers (Re ≤ 500,000 for a flat plate [12]) in the injectors result in a larger displacement thickness, effectively reducing the nozzle area. At higher chamber pressures the ratio approaches unity, indicating smaller displacements in turbulent regimes. To predict the performance of a manufactured injector including boundary layer blockage, the effective area is used in place of the design area[1].

The shear stress is also significant in micro channels, modeled here by integrating the drag force along the differential wetted area in the streamwise direction

$$F_{drag} = \int C_f \frac{1}{2} \rho u^2 dA_{wet} \qquad (4)$$

where

$$C_f = \frac{f}{4} = \frac{C}{4} Re^{-m} \qquad (2)$$

The constants C and m are found from Incropera [14] for laminar entry, laminar, and turbulent flow regimes. The drag force in the combining cone and motive nozzle is plotted in Fig. 5 as a function of chamber pressure. Similar to the boundary layer blockage, F_{drag} becomes less significant as the Reynolds number increases.

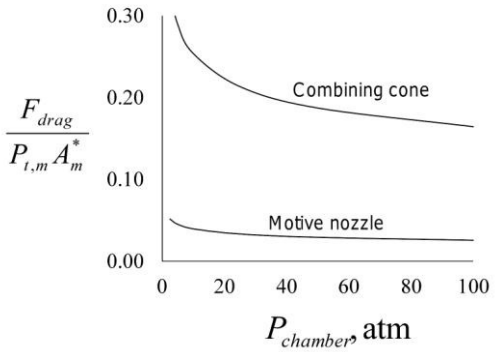

Fig. 5: Normalized drag force versus chamber pressure.

EXPERIMENTAL SETUP

To validate the model that now includes boundary layer blockage and friction losses, a micro injector was fabricated and tested using steam to pump ethanol. The injector was machined from three stainless steel plates bolted together, and the assembly was connected to a boiler that would supply the motivating steam and a tank that stored the suction liquid (ethanol). The test piece includes the restrictor, motive nozzle and combining cone; the delivery cone is modeled as a diffuser so that $P_{t,discharge} = \pi_{diff} P_{t,d}$.

The ethanol tank was maintained at near-ambient pressure and at temperatures near 200 K. The pressure of the supplied steam would be varied between 3 and 12 atm during the experiment. A schematic of the experimental set-up is shown in Ref [9].

To begin the experiment the valve from the ethanol tank to the injector is opened, allowing the suction liquid to fill the reservoir. Once the water in the boiler has reached saturation at the desired $P_{t,m}$ the valve to the injector is opened, forcing the motive vapor into the nozzle where the resulting low-pressure region draws the suction liquid into the combining cone. A needle valve controlling the pressure from the boiler is tuned until the system reaches steady-state operation, identified by a condensed liquid discharge stream.

The measured output pressure was obtained by attaching a polypropylene "cantilever" to the top of the injector, which was deflected by the discharge stream. The deflection of the cantilever was measured once the injector had achieved steady-state operation and classic beam theory was used to compute the injector output pressure from the measured deflection as outlined by Ref [9].

RESULTS AND DISCUSSION

At the motive pressures of interest, Figs. 4 and 5 show that the influence of the viscous boundary layer cannot be neglected, implying that a detailed and accurate loss model is necessary to predict the injector performance within this operating range. To compare the loss model developed to the experimental results,

[1]Only the effective combining cone area is substituted into the final model since $A_{eff}/A \geq 95\%$ for the motive nozzle of each injector at the chamber pressures of interest.

the measured discharge pressure is compared to the predicted pressure. Table 1 shows the quantities measured during the experiment.

Table 1: Quantities measured during experiment

		Run					
		1	2	3	4	5	6
$P_{t,m}$	atm	3	5.4	6.8	8.8	9.8	11.9
P_{tank}	atm	1.3 for all runs					
P_s	atm	1 for all runs					
$T_{t,s}$	K	337	338	338	350	331	353
Δ	mm	3.5	4.5	5	5.5	5	6

A comparison of the model to the experimental results is shown in Fig. 6. The pressure ratio across the injector is plotted as a function of the supplied pressure. It is noted that the experiment and theory agree within 15% overall and that the injector is capable of delivering a discharge pressure (less the pressure of the suction liquid) up to twice that of the supplied motive pressure. As the supplied pressure is increased, the pressure ratio across the injector decreases for a constant-area injector.

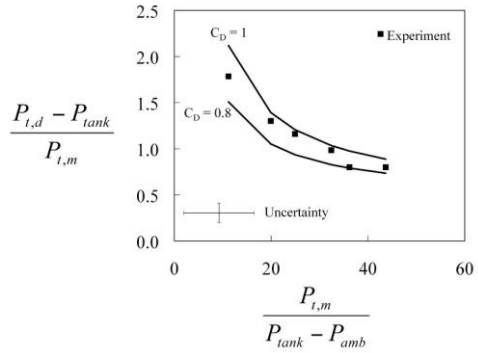

Fig. 6: Injector experimental results showing comparison with model and the average uncertainty.

Possible sources of error during the experiment include device measurement inaccuracies such as pressure gauge readings and the measurement of the cantilever deflection; the limitations of beam theory; and the difficulty in distinguishing between steady-state and almost-steady-state operation.

CONCLUSION

The proposed engine cycle incorporates injectors for pumping the propellants from their tanks in such a way that the chamber pressure is equal to the discharge pressure, less any pressure drop across the manifold plate, as shown by Eq. (1). Because nearly all performance and design parameters of a rocket engine are functions of $P_{chamber}$, accurately modeling the injectors is crucial to the engine design and performance calculations.

The small length scale of the engine implies low-Reynolds number flow through high aspect ratio micro channels, especially through the injectors, resulting in increased boundary layer interactions. In the combining cone for example, results showed that for $P_{t,m}$ = 10 atm, the exit area is effectively reduced by 25% and C_{drag} is 0.29. By studying these effects, a greater understanding of the fluid behavior in the injectors is developed, eliciting a more accurate engine design.

REFERENCES

[1] Brikner NA, Gardner WG, Wang I, Protz JM 2010 A Study and Design of a Giffard Injector-Pumped Bipropellant Microrocket Proceedings of 57th JANNAF JPM 2010 (Colorado Springs, CO 3-7 May 2010)

[2] Brikner NA 2010 Modeling and Analysis of a Giffard Injector-Pumped Bipropellant Microrocket Duke Un*iversity master's thesis*

[3] Giffard H 1860 Improved Feed-Water Apparatus for Steam-Boilers US Patent #27,979 1860

[4] Nissenson GN 1890 Practical Treatise on Injectors as Feeders of Steam Boilers (Published by the author)

[5] Kneass SL 1920 Practice and Theory of the Injector (New York, John Wiley and Sons, Inc.)

[6] London AP 1995 A Systems Study of Propulsion Technologies for Orbit and Attitude Control of Microspacecraft Massachusetts Institute of *Technology master's thesis*

[7] Protz CS 2004 Experimental investigation of microfabricated bipropellant rocket engines Massachusetts Institute of Technology PhD disseration

[8] Marcu B, Prueger G, Epstein AH, Jacobsen SA 2005 The commoditization of space propulsion: Modular propulsion based on MEMS technology Proceedings of AIAA JPC 2005 (Tucson, AZ 10-13 July 2005)

[9] Gardner WG, Wang I, Brikner NA, Jaworski JW, Protz JM 2010 Experimental Results and Modeling for a Microfabricated Giffard Jet Injector J. Micromech. Microeng. (under review)

[10] Brikner NA, Protz JM 2010 A Design of a Giffard Injector-Pumped Bipropellant Microrocket Proceedings of AIAA JPC 2010 (Nashville, TN 25-28 July 2010)

[11] Brikner NA, Gardner WG, Shen HS, Protz, JM 2010 Investigation of Heat Transfer and Scale Effects on the Performance of a Giffard Injector-Pumped Microrocket J. Thermal Sciences and Engineering Applications (under review)

[12] Cengel YA, Ghajar AJ 2011 Heat and Mass Transfer: Fundamentals and Applications (New York, McGraw-Hill 4th edition)

[13] Greitzer EM, Tan CS, Graf MB 2004 Internal Flow (New York, Cambridge University Press)

[14] Incropera FP, Dewitt DP, Bergman TL, Lavine AS 2007 Fundamentals of Heat and Mass Transfer (John Wiley & Sons)